IEEE Catalog Number
CFP1292L-USB
ISBN 978-1-4673-1371-1

IEEE

Advanced iron-loss calculation as a basis for efficiency improvement of electrical machines in automotive application

Simon Steentjes, Marc Leßmann, and Kay Hameyer
Institute of Electrical Machines, RWTH Aachen University
Germany, 52056 Aachen, Schinkelstr. 4
Corresponding author: simon.steentjes@iem.rwth-aachen.de

***Abstract*—The accurate prediction of iron losses of soft magnetic materials for various frequencies and magnetic flux densities is eminent for an enhanced design of electrical machines in automotive applications. For this purpose different phenomenological iron-loss models have been proposed describing the loss generating effects. Most of these suffer from poor accuracy for high frequencies as well as high values of magnetic flux densities. This paper presents a comparison of the common iron-loss models to an advanced iron-loss formula. The proposed *IEM-Formula* resolves the limitation of the common iron-loss models by introducing a high order term of the magnetic flux density. Exemplarily, the iron-loss formula is utilized to calculate the iron losses of an induction machine for the drive train of a full electric vehicle.**

I. Introduction

In the ongoing climate debate, the electrification of transportation represents a promising approach to reduce CO_2 as well as pollutant emissions and to become increasingly independent of fossil energy carriers. The development of fully electrified (EV, electrical vehicle) and hybrid vehicles (HEV, hybrid electrical vehicle) represents a great potential in order to come closer to this goal, and is an important alternative to the traditional, combustion engine powered vehicles. Due to the strong limitation of the batteries capacity up to date, the optimization of electrical machine's efficiency for various operating points and operation modes ranks first. The efficiency improvement of rotating electrical machines – whether they are high power motors/generators, traction motors for electrical/hybrid vehicles, and/or smaller power motors in appliances – is and has always been a key driver in the electrical steel market, pushing the material choice towards electrical steel grades with lower intrinsic iron losses. This is not only triggered by the objective to reduce operational costs by downsizing the energy dissipation during the electromechanical energy conversion, but also to comply with more and more stringent worldwide regulations concerning energy efficiency, for instance as stipulated by the IEC standard 60034-30 efficiency classes for asynchronous motors. In addition, the emerging market of electrical and hybrid vehicles is boosting intensively the research in highly efficient electrical drive systems, for which in particular electrical machines are demanded with high torque densities (which means high torque production with low weight motors) in wide speed ranges, and with elevated operating frequencies, typically within the range $200 - 800\,\mathrm{Hz}$, i.e. well above the power line frequency.

For the development and electromagnetic design of these high efficiency electrical machines there is a strong need for improved and more accurate iron-loss models. Due to the increasing motor speed, requiring field weakening operation, a wide operational range of frequency f and magnetic flux density B – in particular for the electrical machines with elevated operating frequencies such as the ones incorporated into hybrid or full-electric drive trains of vehicles – is required. The inverter supply with pulse-width modulation additionally induces higher harmonics into the machine causing further losses, which have to be considered. Such improved iron-loss estimation for losses occurring in the machine's stator and rotor is indispensable in order to effectively carry out electromagnetic and thermal design. Therefore the development of enhanced iron-loss estimation models for wide range of magnetic flux density B and frequency f is eminent for increasing the machine performance and efficiency. Accurate loss calculation forms the basis for the selection of the most appropriate electrical steel grade which suits best the specific working conditions in the rotating electrical machine. Moreover, such a development gives more insight in the specific trade-offs that are made during the machine design process of such devices in order to identify the particular specifications of electrical steels, which could be further developed for specific applications.

This paper presents a modified iron-loss model that is derived from the well-known classical Bertotti formulation [1]. Purpose is to better suit the experimentally observed iron-loss characteristics at high magnetic flux density levels by including a term depending on a power of magnetic flux density B which is higher than two (B^2 is the power of the classical Foucault eddy current losses [2]). This model is extended to further consider rotational losses and higher harmonics. For verification a comparison of this model to unidirectional standard and non-standard measurements is performed and an example of use in an induction machine is given.

II. Iron-loss modeling

According to the well-known loss-separation principle [1], the iron losses in electrical steel laminations can be split up into three parts:

1) the Foucault eddy current losses, calculated in a macroscopic way with Maxwell's equations [1], [2],
2) the hysteresis losses, and
3) the excess losses, associated with the presence of domains, leading to various space-time dependencies in the magnetization process [1].

In general, the iron losses in soft magnetic materials are measured and theoretically estimated under specific, standardized conditions such as the Epstein test under uniaxial and purely sinusoidal magnetic flux density at $50\,\mathrm{Hz}$ and $1.0\,\mathrm{T}$, respectively $1.5\,\mathrm{T}$ [3]. However, magnetic flux paths occurring in rotating electrical machines are more complex than in the case of standardized material characterization of the Epstein-strips. Thus, the actual iron losses occurring in electrical machines cannot be placed in a simple relationship to the Epstein loss data. In addition, these approaches are insufficient if new machine designs with higher material utilization are introduced (higher peak values of the magnetic flux density B) and higher operating frequencies f are attained.
Additional reasons for this lack of accuracy could be summarized as follows:

- harmonics of the magnetic flux waveform due to iron saturation, skin effect, stator and rotor slots, harmonics in excitation and supply currents (e.g. pulse-width modulation),
- the rotating electrical machine has important differences compared to the standardized conditions of the Epstein-test such as geometry and non-unidirectional magnetization conditions, resulting in rotational losses,
- changes in the magnetic properties of the material during the production process due to residual stresses and applied stresses such as cutting effects.

Therefore, these parasitic effects should be considered and included in the iron-loss calculation to more accurately predict the iron losses. Up to a certain degree this is aimed in the proposed improved iron-loss model.

A. Classical Bertotti iron-loss model

Bertotti derived, based on a low-frequency limit, an equation to calculate the iron losses considering the loss-separation principle [1]:

$$P_{Fe} = k_{hyst}^{'} \cdot \hat{B}^{\alpha} f + k_{classic}^{'} \cdot \hat{B}^{2} f^{2} + k_{excess}^{'} \cdot \hat{B}^{1.5} f^{1.5}, \quad (1)$$

with $k_{classic}^{'} \equiv \frac{\pi^2 d^2}{6\rho\rho_e}$ and $k_{hyst}^{'}, k_{excess}^{'} \hat{=}$ constant. The first term represents the hysteresis losses, the second term the classical Foucault eddy current losses [2] and the latter the excess losses, where:

- $\hat{B}$: Peak magnetic flux density in Tesla $[T]$,
- α: Exponential coefficient of hysteresis losses,
- f: Fundamental frequency in Hertz $[Hz]$,
- d: Thickness of the steel lamination in meter $[m]$,
- ρ: Mass density of the steel grade in kilogram per cubic meter $[kg/m^3]$,
- ρ_e: Specific electric resistance in Ohm meter $[\Omega m]$,
- P_{Fe}: Total estimated iron losses of the model in Watt per kilogram $[W/kg]$.

It should be noted that the classical Foucault eddy current loss term in (1) is only a simplified description, valid under conditions where the magnetic field H inside a thin lamination sheet shows only a little deviation from the applied magnetic field H_a, i.e. $H \approx H_a$ [1].
A variant of this classical Bertotti description is given in equation (2):

$$P_{Fe} = k_{hyst} \cdot \hat{B}^{\alpha} f + k_{classic} \cdot \hat{B}^{2} f^{2} + k_{excess} \cdot \hat{B}^{1.5} f^{1.5}. \quad (2)$$

This slightly modified approach also uses the classical Bertotti formula (1), but now with all k-parameters fitted to measurements instead of using a calculated value for $k_{classic} = k_{classic}^{'}$ as is described in equation (1).
Bertotti's original approach does not consider rotational losses and harmonics, i.e. it is expected that the estimated loss values are smaller than the real losses. These limitations emphasize the need to expand the existing loss approach to describe the previously mentioned effects additionally contributing to the iron losses.

B. Extended loss model

Epstein measurements are performed under uniaxial (in space) and sinusoidal (in time) magnetic flux density. Thus, magnetic flux density in Epstein frame measurements is completely represented by its fundamental wave. However, in rotating electrical machines this is not the case: higher harmonics (in time) due to iron saturation, skin effect, slotting effect and the use of a power electronics supply (inverter, PWM) can occur, as well as vector magnetic fields (in space), the latter giving rise to so-called rotational losses.
In order to improve common iron-loss models to these conditions, rotational losses and higher harmonics in each part, i.e. in each finite element of stator and rotor lamination, have to be considered by:

- A Fourier analysis of the magnetic flux density waveform during the least common multiple of electrical period length and rotational period of rotor to identify the higher harmonics [4], [5], [6];
- The level of magnetic flux distortion and the saturation. Two parameters B_{min} and B_{max}, respectively the minimal and maximal magnetic flux density amplitudes over time, serve for this. This enables to identify the level of magnetic flux distortion by taking the ratio between B_{min} and B_{max}.
  B_{max} gives an idea about the level of saturation. Zones with rotational hysteresis are those with large values of B_{min}, whereas unidirectional field corresponds with a zero value of amplitude B_{min}.

In the accentuated loci (Figure 1) of the stator laminations, the different magnetization types can be found. The diagram of

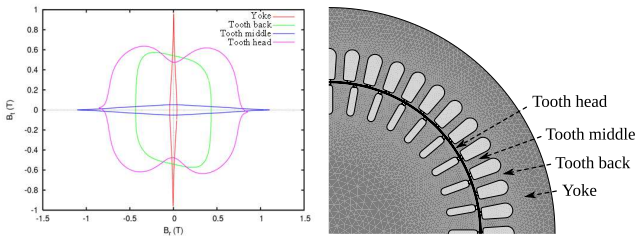

Fig. 1: Flux distortion (described in tangential B_t and radial B_r coordinates) at different points of the machine as indicated on the right.

Figure 1 indicates that there are unidirectional magnetizations in the middle of the teeth, whereas elliptical up to nearly circular magnetizations can be found at the back and head of teeth.
The incorporation of the aforementioned effects leads to the following extended iron-loss formula [4], [5], [6]:

$$\begin{aligned} P_{Fe} = {} & k_{hyst} \cdot \left(1 + \frac{B_{min}}{B_{max}} \cdot (r_{hyst} - 1)\right) \cdot \hat{B}^{\alpha} \cdot f \\ & + k_{classic} \cdot \sum_{n=1}^{\infty} \left(\hat{B}_n^2 \cdot (nf)^2\right) \\ & + k_{excess} \cdot \left(1 + \frac{B_{min}}{B_{max}} \cdot (r_{excess} - 1)\right) \\ & \cdot \sum_{n=1}^{\infty} \left(\hat{B}_n^{1.5} \cdot (nf)^{1.5}\right), \end{aligned} \tag{3}$$

with $\hat{B}_n = \sqrt{\hat{B}_{n,x}^2 + \hat{B}_{n,y}^2}$. Thereby $\hat{B}_{n,x}$ and $\hat{B}_{n,y}$ represent the amplitude of the n-th harmonic in x- and y- direction, whereas the origin of the coordinate system is defined in the center of the machine. The first term represents the hysteresis loss and includes the flux distortion factor $c \equiv \frac{B_{min}}{B_{max}}$, as well as the rotational loss factor r_{hyst}. Considering the flux distortion factor, arbitrary spatial flux density loci like the ones shown in Figure 1, or pure rotational ($c = 1$, which means $B_{min} = B_{max}$) can be described. The second term considers the classical Foucault eddy current losses and takes harmonics into account. Hereby a summation over all n harmonics is conducted. The same is performed for the third, the excess loss term. r_{excess} describes the rotational excess losses.
Instead of Cartesian coordinates any perpendicular coordinate system could be chosen, like a cylindrical one as shown in Figure 1. Three different ways to identify the k-parameters exist.

- By least-square fitting all three k-parameters towards loss measurements, or
- by explicitly calculating $k_{classic} = \frac{\pi^2 d^2}{6\rho\rho_e}$ and fitting the two remaining parameters, or
- physical identification of all the k-parameters.

C. 5-Parameter-IEM-Formula

It has been determined in [7], [8] and [9] that the classical Bertotti model (1, 2) underestimates the losses at high magnetic flux densities and high frequencies due to the neglection of saturation losses. To overcome this, the IEM proposed and validated a fourth loss term with a higher order B dependence (which means higher than B^2 for the classical Foucault eddy current losses).
The proposed mathematical formulation with higher order B term reads as follows:

$$P_{Fe} = a_1 \hat{B}^2 f + a_2 \hat{B}^2 f^2 \left(1 + a_3 \hat{B}^{a_4}\right) + a_5 \left(\hat{B} f\right)^{1.5}, \tag{4}$$

where:

- $\hat{B}$: Magnetic flux density in Tesla [T]
- f: Fundamental frequency in Hertz [Hz]
- a_i: Fitted material parameters

Hysteresis losses, classical Foucault eddy current losses and excess losses are included (respectively as terms with a_1, a_2 and a_5 coefficients), as well as the additional higher order B term, $a_3 B^{a_4}$. In the first instance, the loss model is only based on the fundamental frequency component and all a-parameters are fitted to Epstein measurements using the least-square method.
However, the three aforementioned descriptions of iron-loss (1 - 4) take each in itself different parasitic effects in electrical machines such as harmonics in time and space, flux distortion and rotational effects as well as material effects (saturation effects) into account. Thus, all these loss models are combined/coupled to obtain a single iron-loss formula, which then contains the most important parasitic effects. This new formulation is called *IEM-Formula*.
The *IEM-Formula* is based on adding analytical descriptions to include the mentioned additional effects:

- The eddy current and excess loss description of the classical Bertotti formula (1, 2) is extended with a summation over all harmonics (3) in order to take the influences of harmonics into account.
- Subsequently the hysteresis and excess loss terms are extended to model the influence of rotational and flux distortion effects on the corresponding losses (3).
  For the time being, the rotational loss factors are a fixed value ($r_{hyst} = r_{excess} = 2.5$). In future they will be implemented as a monotonous decreasing function of the magnetic flux density. However, additional studies on the rotational behavior of loss are necessary to take it a step further.
- Finally the influence of the nonlinear magnetization behavior at higher magnetic flux densities is included using an additional higher order term in B (4).

This results in the following description, the *IEM-Formula*:

$$P_{Fe} = P_{hyst} + P_{classical} + P_{excess} + P_{sat} \tag{5}$$

with the following loss contributions:

$$P_{hyst} = a_1 \cdot \left(1 + \frac{B_{min}}{B_{max}} \cdot (r_{hyst} - 1)\right) \cdot \hat{B}^2 \cdot f \tag{6}$$

$$P_{classical} = a_2 \cdot \sum_{n=1}^{\infty} \left(\hat{B}_n^2 \cdot (nf)^2\right) \tag{7}$$

$$P_{excess} = a_5 \cdot \left(1 + \frac{B_{min}}{B_{max}} \cdot (r_{excess} - 1)\right) \cdot \sum_{n=1}^{\infty} \left(\hat{B}_n^{1.5} \cdot (nf)^{1.5}\right) \tag{8}$$

$$P_{sat} = a_2 \cdot a_3 \cdot \hat{B}^{a_4+2} \cdot f^2 \tag{9}$$

For that, $\hat{B}$ is the amplitude of the fundamental frequency component of the flux density in Tesla $[T]$, $\hat{B}_n$ the amplitude of the n-th harmonic component of the magnetic flux density in Tesla $[T]$, n the order of harmonic, f the fundamental frequency in Hertz $[Hz]$, $a_1 - a_5$ the material specific parameters and r_{hyst}, r_{excess} the rotational loss factors.

III. Comparison to standardized measurements

The parameters $a_1 - a_5$ used in (4 - 9) are identified on the one hand by a pure mathematical fitting procedure performed on the measured data sets and on the other hand by a semi-physical identification procedure. The latter is explained below.

As part of the semi-physical parameter identification, firstly the parameter a_1, describing the hysteresis losses, is determined by means of dc-loss measurements (quasi-static loss measurements) at a standard Epstein frame. The sheet metal strips of the soft magnetic material are uniformly distributed in accordance with the rolling direction, i.e. strips cut along and perpendicular to the rolling direction with dimensions of $280\,\mathrm{mm}$ x $30\,\mathrm{mm}$ are used. Measurements are performed with sinusoidal uniaxial magnetic flux densities.

The parameter a_2 for the classical Foucault eddy current losses is calculated by the macroscopic equation

$$a_2 = \frac{\pi^2 d^2}{6 \rho \rho_e}, \tag{10}$$

with the sheet thickness d, the material specific density ρ and the specific electrical resistivity ρ_e of the soft magnetic material.

The excess loss parameter a_5 is identified by measurements at rather low frequencies between $5\,\mathrm{Hz}$ and $10\,\mathrm{Hz}$. In this frequency range, the magnetic field origintaing from the macroscopic eddy currents can be neglected compared to the applied magnetic field. Hence, the excess loss term is easily separated.

The parameters a_3 and a_4 are determined from the nonlinear material behavior at high frequencies and magnetic flux densities [9]. Thus, the measurements to identify a_3 and a_4 are performed in a frequency range from $500\,\mathrm{Hz}$ to $2000\,\mathrm{Hz}$ on two Epstein frames with sinusoidal uniaxial magnetic flux densities in a wide modulation range. Here, the non-grainoriented electrical steel grade M270-35A is studied.

TABLE I: Mathematical identified parameter sets

	k_{hyst}	$k_{classic}$	k_{excess}	α	
Eq. (2)	0.01525	$98.56 \cdot 10^{-6}$	$70.0 \cdot 10^{-6}$	2	
	a_1	a_2	a_5	a_3	a_4
Eq. (4)	0.00989	$26.39 \cdot 10^{-6}$	$0.89 \cdot 10^{-3}$	0.19	5.15

TABLE II: Semi-physical identified parameter sets

	k'_{hyst}	$k'_{classic}$	k'_{excess}	α	
Eq. (1)	0.0117	$50.34 \cdot 10^{-6}$	$446.67 \cdot 10^{-6}$	1.9990	
	a_1	a_2	a_5	a_3	a_4
Eq. (4)	0.0117	$50.34 \cdot 10^{-6}$	$446.67 \cdot 10^{-6}$	0.1	4.2965

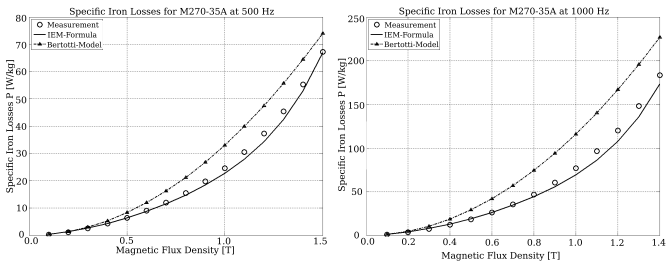

Fig. 2: Comparison of the 5-Parameter-IEM-Formula (4) to measurements and the Bertotti-Formula (2) for M270-35A at a frequency of $500\,\mathrm{Hz}$ (left) and $1000\,\mathrm{Hz}$ (right) using the parameters obtained from mathematical fitting.

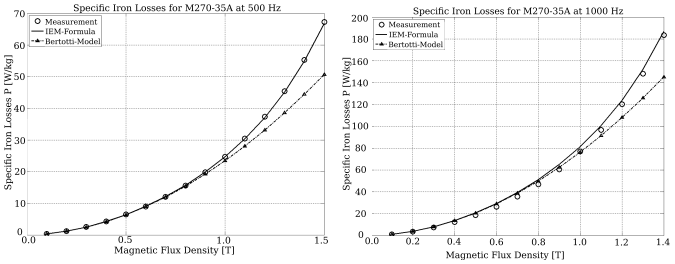

Fig. 3: Comparison of the 5-Parameter-IEM-Formula (4) to measurements and the Bertotti-Formula (2) for M270-35A at a frequency of $500\,\mathrm{Hz}$ (left) and $1000\,\mathrm{Hz}$ (right) using the semi-physical parameters.

Table I presents the resulting parameters obtained by the mathematical fitting and Table II the ones obtained using the semi-physical identification procedure. Using these parameters the predicted iron losses by the classical Bertotti model (1, 2) and the IEM-5-Parameter-Formula (4) are compared to each other (Figure 2, 3). Equation (1, 2) and (4) are sufficient for this first comparison since standardized measurements impress/control a purely sinusoidal uniaxial magnetic flux density across the lamination thickness. Thus, proposed extensions for harmonics need not to be considered. Regarding to Figure 2 it is obvious that the Bertotti model (2) overestimates the iron losses for both presented frequencies using the mathematically identified

parameters (Table I). The IEM-5-Parameter-Formula describes the loss behavior accurately.
Using semi-physical parameters leads to significantly different loss predictions. The Bertotti model (1) underestimates the iron losses at high magnetic flux densities for both presented frequencies (Figure 3), whereas the IEM-5-Parameter-Formel describes the loss behavior accurately using the high order term in B (4).

IV. Comparison to non-standard measurements

The *IEM-Formula* is compared to non-standard measurements, i.e. measurements with harmonic contents imposed in the magnetic flux density waveform. The used parameter set consists of the one identified under sinusoidal uniaxial magnetic flux density conditions. The Epstein measurement results in an experimental iron-loss value corresponding with the non-sinusoidal magnetic flux density waveform. On the other hand, the *IEM-Formula* (5) is applied to these conditions by the given values for the harmonics' frequencies and the amplitudes, giving rise to a calculated iron-loss value, which then can be benchmarked against the experimental value. With this method the accuracy and reasonability of the model extensions for higher harmonics and the additional effects in the IEM-Formula are studied in detail. Calculated iron losses are compared with measurements at 400Hz fundamental frequency and two different magnetic flux density amplitudes with harmonics of the order 5 and 9 (Figure 4, 5).

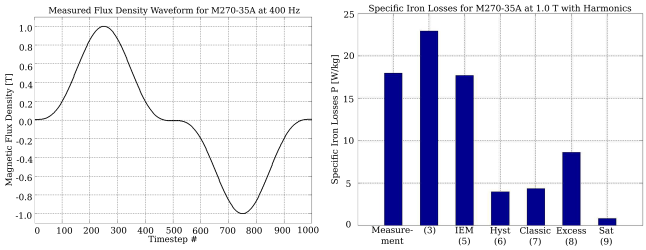

Fig. 4: Comparison of the *IEM-Formula* (5) and the Extended loss model (3) to non-standard measurements at a fundamental frequency of 400 Hz and magnetic flux density of 0.78 T (right). On the left the used magnetic flux density waveform is shown.

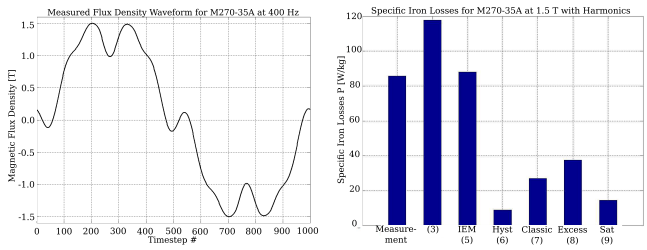

Fig. 5: Comparison of the *IEM-Formula* (5) and the Extended loss model (3) to non-standard measurements at a fundamental frequency of 400 Hz and magnetic flux density of 1.5 T (right). On the left the used magnetic flux density waveform is shown.

The presented resulting losses for different flux density waveforms, calculated as well as measured, emphasize the accuracy of the developed loss model. The accuracy is increasing for ascending flux density amplitudes. The model predicts the iron losses in the saturation region with a deviation of less than 2%, in the linear region of the single-valued curve the deviation is less than 4%. Furthermore the model predicts the loss values with the same accuracy for different amounts of harmonics. Although it is a rather mathematical model, the results obtained serve as a first validation of the higher harmonic term in the *IEM-Formula*.

V. Induction machine loss analysis

The *IEM-Formula* is exemplarily employed to an induction machine model. Single-valued magnetization curves have been used to consider saturation effects originating from the non-linear material behavior. Second-order effects, originating from hysteresis behavior, are neglected. Pure hysteresis, classical Foucault eddy current, excess as well as saturation losses in the laminated stator and rotor cores are estimated a posteriori using the local waveforms of the magnetic flux densities in (5).
The cross section of the laminated stator and rotor core of the 8 pole induction machine under consideration is shown in Figure 1. To reduce the 5th and 7th harmonic, a distributed and chorded winding with 5/6 pitch is used. Transient 2-D computations of the field distribution have been performed by in-house FE-solver *iMOOSE* [10]. The magnetic flux density distribution for one simulation step at nominal operation is shown in Figure 6. The iron losses of the studied induction machine are calculated in the post process of the FE-simulation by adapting the *IEM-Formula* (5) on the least common multiple of electrical period length and rotational period of rotor (Figure 7, 8 and 9). Figure 10 presents the distributions of B_{max} and B_{min} serving as a basis for determination of the level of saturation and magnetic flux distortion.
The numerical simulation of an induction machine reveals the following physical phenomena: 1) Magnetic saturation in the tooth middle and head, 2) significant rotational flux in the back of tooth, 3) high harmonic pulsations in the local flux waveforms due to stator and rotor slots as well as saturation effects.

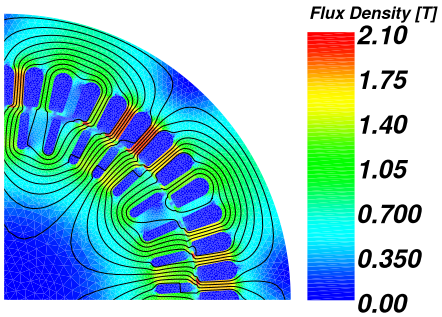

Fig. 6: Magnetic flux density distribution of the investigated induction machine.

As shown in Figure 7 and 8, the main contribution to each fraction of total specific losses occurs in the magnetically high exploited stator teeth at nominal rotor speed of $n = 5925\,\mathrm{min}^{-1}$. The ratio $\frac{B_{min}}{B_{max}}$, indicating rotational flux, is identified by observing the amount of minimal and maximal flux density for each finite element of the yoke. Areas of high rotational flux can be found in the back of tooth, inducing increased rotational hysteresis losses in these regions of yoke (Figure 7 and 10). The excess and saturation losses mainly occur in regions of high flux densities (head of stator and rotor tooth, middle of stator tooth), whereas an additional appearance of excess losses can be found in the back of stator teeth. Due to the comparatively low rotor flux density and frequency of fundamental, the rotor losses are mainly limited to the rotor teeth, induced by harmonics of stator and rotor slots.

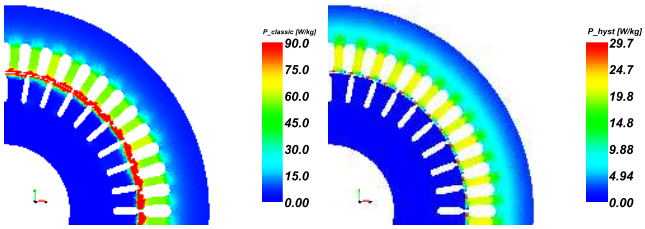

Fig. 7: Illustration of the classical Foucault eddy current loss (left) and hysteresis loss (right) distribution of the investigated induction machine for iron-loss calculation with (5).

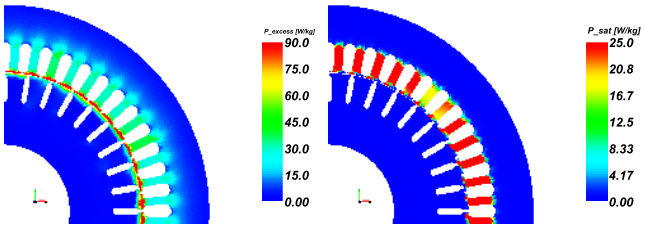

Fig. 8: Illustration of the excess loss (left) and saturation (high order) loss (right) distribution of the investigated induction machine for iron-loss calculation with (5).

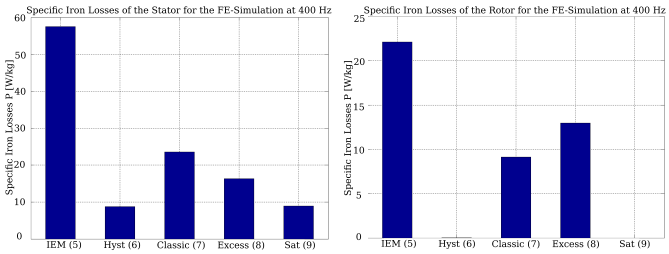

Fig. 9: Visualization of the loss contributions of stator and rotor of the investigated induction machine for iron loss calculation with (5).

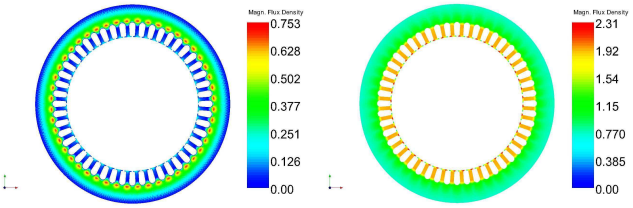

Fig. 10: B_{min} (left) and B_{max} (right) distribution.

VI. Conclusion

This paper presents a modified iron-loss model for the accurate iron-loss estimation under non ideal magnetization conditions. The model considers harmonics as well as rotational magnetization and saturation effects. The accuracy of the computed iron losses for harmonics under saturation is shown by the comparison of simulations to measurements under non-sinusoidal excitations at an Epstein frame. The model of an induction machine is taken as an example to calculate the iron losses. Commonly used iron-loss models are insufficient at high magnetic flux densities and frequencies, resulting in the need for advanced iron-loss formulas. Such improved iron-loss estimation is indispensable for increasing the machine performance and efficiency. Consequently, this forms the basis for the selection of the most appropriate electrical steel grade which suits best the specific working conditions in the rotating electrical machine and gives insight in the specific trade-offs that are made during the machine design process of such devices. Thus, particular requirements on electrical steel for specific applications can be identified for further steel development.
Additional studies regarding the influence of minor loops and the rotational loss behavior will be conducted in the next steps of this research work.

References

[1] G. Bertotti, *Hysteresis in Magnetism: For Physicists, Materials Scientists, and Engineers*, Academic Press, 1998.

[2] J. Lammeraner and M. Stafl, *Eddy Currents*, Iliffe, 1967.

[3] IEC 404-2 and IEC 404-3.

[4] G. Bertotti, A. Canove, M. Chiampi, D. Chiarabaglio, F. Fiorillo and A.M. Rietto, "Core loss prediction combining physical models with numerical field analysis," *J. Magn. Magn. Mat.*, vol. 133, pp. 647-650, 1994.

[5] F. Fiorillo and A. Novikov, "An Improved Approach to Power Losses in Magnetic Laminations under Nonsinusoidal Induction," *IEEE Trans. Magn.*, vol 26, no. 5, 1990.

[6] F. Fiorillo and A. Novikov, "Power losses under sinusoidal, trapezoidal and distorted induction waveform," *IEEE Trans. Magn.*, vol. 26, no. 5, pp. 2559 - 2561, 1990.

[7] S. Jacobs, D. Hectors, F. Henrotte, M. Hafner, K. Hameyer, P. Goes, D. Ruiz Romera, E. Attrazic, S. Paolinelli, "Magnetic material optimization for hybrid vehicle PMSM drives," *Inductica conference*, Chicago (USA), 2009.

[8] D. Schmidt, M. van der Giet and K. Hameyer, "Improved iron-loss prediction by a modified loss-equation using a reduced parameter identification range," *Proc. Conf. Soft Magn. Mat.*, SMM20, p. 421, Kos (Greece), 2011.

[9] D. Eggers, S. Steentjes and K. Hameyer, "Advanced iron-loss estimation for nonlinear material behavior," *IEEE Trans. Magn. (in press).*

[10] [Online] Institute of Electrical Machines, *www.iem.rwth-aachen.de*, 26.07.2012.